AD-A255 475

Public reporting bu
gathering and mail
collection of inforn
Davis Highway, Sui

...esponse, including the time for reviewing instructions, searching exis..ng da.. s..rces,
..formation. Send comments regarding this burden estimate or any o..er a.. thi..
..quarters Services, Directorate for Information Operations and Report.. 121.. Jeffers..
..udget, Paperwork Reduction Project (0704-0188), Washington, DC 205..

1. AGENCY U		3. REPORT TYPE AND DATES COVERED

4. TITLE AND SUBTITLE	5. FUNDING NUMBERS
Transmission coefficient measurement and improved sublayer material property determination for thick underwater acoustic panels: A generalization and improvement of the ONION method	PE - 61153N TA - RR011-08-42 WU - DN220-161

6. AUTHOR(S)

Jean C. Piquette

7. PERFORMING ORGANIZATION NAME(S) AND ADDRESS(ES)	8. PERFORMING ORGANIZATION REPORT NUMBER
Naval Research Laboratory Underwater Sound Reference Detachment P.O. Box 568337 Orlando, FL 32856-8337	

9. SPONSORING/MONITORING AGENCY NAME(S) AND ADDRESS(ES)	10. SPONSORING/MONITORING AGENCY REPORT NUMBER
Office of Naval Research 800 N. Quincy Street Arlington, VA 22217-5000	

DTIC
ELECTE
AUG 3 1992
S
A
D

11. SUPPLEMENTARY NOTES

12a. DISTRIBUTION/AVAILABILITY STATEMENT	12b. DISTRIBUTION CODE
Approved for public release; distribution unlimited	

13. ABSTRACT *(Maximum 200 words)*

Modifications of the ONION panel-measurement method that allow for simultaneous analysis for transmitted- and reflected-wave data are described. The revised algorithm determines more reliable values for the sound speed and loss of the material of each panel sublayer than does the algorithm that is based exclusively upon analysis of the reflected wave. Included in the revised method is a Taylor series expansion of the sound-speed function of each layer about the steady-state driving angular frequency. This Taylor series is similar to that used for the loss function in the original ONION method, and is introduced here to more accurately accommodate the frequency variation of the phase speed than does the frequency-independent model used previously. Descriptions of successful applications of the revised ONION method to experimental data are provided. The version of the ONION method described in this report has recently been adopted as the standard panel measurement method at the Underwater Sound Reference Detachment of the Naval Research Laboratory (NRL-USRD) in Orlando, FL for tests conducted in the 1- to 20-kHz frequency interval.

14. SUBJECT TERMS		15. NUMBER OF PAGES
Panel measurements Reflection and scattering	Materials measurements methods	10
		16. PRICE CODE

17. SECURITY CLASSIFICATION OF REPORT	18. SECURITY CLASSIFICATION OF THIS PAGE	19. SECURITY CLASSIFICATION OF ABSTRACT	20. LIMITATION OF ABSTRACT
UNCLASSIFIED	UNCLASSIFIED	UNCLASSIFIED	UL

GENERAL INSTRUCTIONS FOR COMPLETING SF 298

The Report Documentation Page (RDP) is used in announcing and cataloging reports. It is important that this information be consistent with the rest of the report, particularly the cover and title page. Instructions for filling in each block of the form follow. It is important to *stay within the lines* to meet *optical scanning requirements*.

Block 1. Agency Use Only *(Leave blank)*.

Block 2. Report Date. Full publication date including day, month, and year, if available (e.g. 1 Jan 88). Must cite at least the year.

Block 3. Type of Report and Dates Covered. State whether report is interim, final, etc. If applicable, enter inclusive report dates (e.g. 10 Jun 87 - 30 Jun 88).

Block 4. Title and Subtitle. A title is taken from the part of the report that provides the most meaningful and complete information. When a report is prepared in more than one volume, repeat the primary title, add volume number, and include subtitle for the specific volume. On classified documents enter the title classification in parentheses.

Block 5. Funding Numbers. To include contract and grant numbers; may include program element number(s), project number(s), task number(s), and work unit number(s). Use the following labels:

C	- Contract	PR	- Project
G	- Grant	TA	- Task
PE	- Program Element	WU	- Work Unit Accession No.

Block 6. Author(s). Name(s) of person(s) responsible for writing the report, performing the research, or credited with the content of the report. If editor or compiler, this should follow the name(s).

Block 7. Performing Organization Name(s) and Address(es). Self-explanatory.

Block 8. Performing Organization Report Number. Enter the unique alphanumeric report number(s) assigned by the organization performing the report.

Block 9. Sponsoring/Monitoring Agency Name(s) and Address(es). Self-explanatory.

Block 10. Sponsoring/Monitoring Agency Report Number. *(If known)*

Block 11. Supplementary Notes. Enter information not included elsewhere such as: Prepared in cooperation with...; Trans. of...; To be published in.... When a report is revised, include a statement whether the new report supersedes or supplements the older report.

Block 12a. Distribution/Availability Statement. Denotes public availability or limitations. Cite any availability to the public. Enter additional limitations or special markings in all capitals (e.g. NOFORN, REL, ITAR).

DOD	- See DoDD 5230.24, "Distribution Statements on Technical Documents."
DOE	- See authorities.
NASA	- See Handbook NHB 2200.2.
NTIS	- Leave blank.

Block 12b. Distribution Code.

--

DOD	- Leave blank.
DOE	- Enter DOE distribution categories from the Standard Distribution for Unclassified Scientific and Technical Reports.
NASA	- Leave blank.
NTIS	- Leave blank.

Block 13. Abstract. Include a brief *(Maximum 200 words)* factual summary of the most significant information contained in the report.

Block 14. Subject Terms. Keywords or phrases identifying major subjects in the report.

Block 15. Number of Pages. Enter the total number of pages.

Block 16. Price Code. Enter appropriate price code *(NTIS only)*.

Blocks 17. - 19. Security Classifications. Self-explanatory. Enter U.S. Security Classification in accordance with U.S. Security Regulations (i.e., UNCLASSIFIED). If form contains classified information, stamp classification on the top and bottom of the page.

Block 20. Limitation of Abstract. This block must be completed to assign a limitation to the abstract. Enter either UL (unlimited) or SAR (same as report). An entry in this block is necessary if the abstract is to be limited. If blank, the abstract is assumed to be unlimited.

Transmission coefficient measurement and improved sublayer material property determination for thick underwater acoustic panels: A generalization and improvement of the ONION method

Jean C. Piquette
Naval Research Laboratory, Underwater Sound Reference Detachment, P.O. Box 568337, Orlando, Florida 32856-8337

Modifications of the ONION panel-measurement method [J. C. Piquette, J. Acoust. Soc. Am. **85**, 1029–1040 (1989)] that allow for simultaneous analysis of transmitted- and reflected-wave data are described. The revised algorithm determines more reliable values for the sound speed and loss of the material of each panel sublayer than does the algorithm that is based exclusively upon analysis of the reflected wave. Included in the revised method is a Taylor series expansion of the sound-speed function of each layer about the steady-state driving angular frequency. This Taylor series is similar to that used for the loss function in the original ONION method, and is introduced here to more accurately accommodate the frequency variation of the phase speed than does the frequency-independent model used previously. Descriptions of successful applications of the revised ONION method to experimental data are provided. The version of the ONION method described in this report has recently been adopted as the standard panel measurement method at the Underwater Sound Reference Detachment of the Naval Research Laboratory (NRL-USRD) in Orlando, FL for tests conducted in the 1- to 20-kHz frequency interval.

PACS numbers: 43.20.Fn, 43.20.Px, 43.30.Sf, 43.60.Gk

INTRODUCTION

The ONION method is a panel measurement technique that is based on least-squares fitting of digitally acquired transient pulsed-waveform data to a multiple-layer panel model.[1] Readers who are unfamiliar with the technique should consult the references for complete descriptions and explanations.

All previous descriptions of applications of the method have involved considerations of only reflected-wave data. The reason that the transmitted wave has not heretofore been included in the analysis is that the problems involved in accommodating the transmitted wave are far more formidable than are those involved in accommodating the reflected wave. The primary difficulty associated with the evaluation of the transmitted wave derives from the very low sound speeds that are characteristic of the samples of interest. (These sound speeds can be less than the sound speed in air.) Thus only a very short portion of the transmitted wave is available for analysis prior to the reception of unwanted interfering waves (such as those originating at the sample edges or those associated with measurement facility wall echo). In addition, since pulsed waveforms are used in the tests of interest, the reflected waveform can be resolved into convenient analysis epochs, in which each layer sequentially contributes to the overall reflected waveform. No such convenient subdivision of the transmitted waveform is possible, since even the earliest portions of the transmitted wave have been influenced by every layer of the panel.

In the present article, an extension of the method to include analysis of transmitted-wave data is described. The extended ONION-method algorithm involves simultaneous least-squares fitting of reflected-wave data and transmitted-wave data to a theoretical panel model. That is, the least-squares calculation which is performed within the extended ONION method determines material properties for each of the panel sublayers that simultaneously minimize the mean-squared error of fit between the model and the data for both the reflected waveform and the transmitted waveform.

In the previous applications[1] of the ONION method to only reflected-wave data, the material properties so determined were considered to be merely "curve-fitting" properties, and not necessarily the true material properties of the sublayers. The material properties determined in the reflected-wave analysis can often be unreliable, especially for layers deep within the panel, due to the fact that the amount of influence that a particular layer may have on the reflected wave can be quite small. Hence, any particular layer might assume a wide range of properties and yet a good least-squares minimization might nonetheless be achieved. However, a transmitted-wave analysis must necessarily involve information for every sublayer of the panel. Thus material properties that simultaneously fit reflected- and transmitted-wave data are expected to be more reliable than those that fit the reflected wave only.

In Sec. I are described certain improvements to the raw-data handling algorithms. In particular, this section describes improvements to the waveform start-point determination algorithms. In Sec. II, modifications that have been made to the theoretical model incorporated in the ONION-

method software are discussed. Experiments conducted to investigate the revised ONION method are discussed in Sec. III. A discussion of why the material properties determined by the revised method are believed to be more reliable than those determined by the original ONION method is given in Sec. IV. Section V gives a summary and the conclusions.

I. WAVEFORM START-POINT DETERMINATION

The theoretical panel model used to evaluate the reflected waveform in the ONION-method algorithm assumes that the reflected-wave pulse has been measured at the interface between the water medium and the panel layer located closest to the source of the interrogating wave. Similarly, the theoretical panel model used to evaluate the transmitted waveform assumes that the transmitted-wave pulse has been measured at the interface between the water medium and the panel layer farthest from the acoustic source. (The last panel layer is usually a steel backing plate.) Since any practical measurement obviously requires an offset between the relevant interface and the detecting hydrophone, the experimental waveforms so acquired must be preprocessed, prior to evaluation by the ONION-method software. We consider the preprocessing of each waveform separately.

A. Reflected waveform

As described in Ref. 1, the reflected waveform is experimentally determined using two different measurements. One measurement involves capturing data in the reflection region of the panel with the hydrophone situated at a 5-cm offset distance from the relevant fluid–panel interface. The waveform so acquired is termed a "total" waveform, since it is actually the sum of two waveforms, viz., the incident waveform plus the reflected waveform. A second measurement involves again capturing a waveform with the detecting hydrophone at the same position as was used in acquiring the total waveform, but in this second measurement the test panel is removed. The waveform acquired by this measurement is termed the "incident" waveform. The reflected waveform is then determined by digitally subtracting, point-by-point, the incident waveform from the total waveform.

The reflected waveform obtained in this way can be considered to consist of two distinct time regions. One region may be considered to be a "quasinull" region, resulting from the point-by-point subtraction of the incident waveform from the total waveform in the time region of these waveforms that is associated with the round-trip travel of sound in water between the detecting hydrophone and the relevant fluid–panel interface. The second time region represents the actual reflected waveform.

The incident and total waveforms in the quasinull time region should ideally be identical, and thus, should subtract to a perfect null. However, due to the unavoidable presence of system noise, and due to experimental difficulties in repositioning the detecting hydrophone at the same location in both measurements, a residual nonzero difference remains. The preprocessing software used in the analysis of the earlier reports[1] determines how much of a time shift is required to make the reflected waveform appear to have been measured

at the relevant interface. This is done by (i) performing a statistical analysis of the noise in the quasinull region and, (ii) comparison of this noisy quasinull portion of the waveform to the initial nonzero portion of the waveform to determine the true start time of the reflected wave. A time shift is then applied to the waveform to eliminate the quasinull region. Of course, this process is necessarily imperfect, and errors in start-point determination of 5–10 data points (at a 4-MHz data measurement rate) using this approach are not uncommon.

In order to improve the reflected waveform start-point determination, a second level of preprocessing of the data is now performed. That is, a second level of preprocessing that takes as input the already shifted waveform produced by the first level of preprocessing described above, and further improves the determination of the start point of the reflected waveform, is performed in the revised version of the software. This second-level preprocessing involves relying upon the accuracy of the phase 1 portion of the original ONION-method algorithm. (See Refs. 1 and 2.)

In summary, the phase 1 portion of the algorithm is the layer-stripping (or "onion-peeling") portion. It involves the use of portions of the reflected waveform that do not include multiple internal reflections, so that the simple theoretical expressions for the reflection and transmission coefficients of two semi-infinite half-spaces in intimate contact are applicable. The new waveform start-point algorithm involves, (i) attempting a candidate time shift of the experimental reflected waveform corresponding to a predetermined discrete number of data points, (ii) applying the phase-1 layer-stripping algorithm to the shifted reflected waveform to deduce an approximate sound speed and loss for the panel layer situated closest to the acoustic source and, (iii) computing a theoretical pulsed waveform, based on the stripped values of the material properties. The root-mean-squared error of fit between the model waveform and the shifted experimental waveform, evaluated up to that point in time at which the first internal reflection is expected to occur, is then computed and stored. Next, another candidate time shift is applied to the experimental reflected waveform, and the above-described calculations are run for the new shift. The second-level preprocessing algorithm proceeds in this manner until it has evaluated and stored root-mean-squared errors-of-fit that correspond to a sequence of candidate shifts that vary in discrete amounts from 1/4 cycle (of the steady-state driving frequency) earlier in time, up to 1/4 cycle later in time, relative to the start point of the waveform produced by the first-level quasinull elimination calculation described above. The shift that produces the least root-mean-squared error of fit is taken to be the correct shift, and this shift is then applied to the experimental reflected waveform and retained. The entire waveform-shifting calculation described here requires approximately 1-CPU min to perform on a DEC Micro-Vax™ 3XXX series workstation computer.

B. Transmitted waveform

The waveform-shifting technique described above for the reflected waveform is not applicable to the transmitted waveform. This is due to the fact, previously mentioned, that

the onion-peeling portion of the algorithm does not produce reliable properties for layers situated deep within the panel. (Unlike the reflected waveform, whose initial data points depend only upon properties of the first panel layer, *all* of the data points of the transmitted waveform depend upon the properties of all panel layers.) Thus the time shift of the transmitted waveform must be effected by a different, and less accurate, method.

An additional difficulty associated with the determination of the time location of the start point of the transmitted wave is caused by the (unknown) time delay associated with the time of flight of the transmitted wave from the front fluid–panel interface (i.e., the interface closest to the acoustic source) to the back fluid–panel interface (i.e., the interface farthest from the acoustic source). This delay is experimentally determined by performing two waveform measurements in the transmission region of the panel. We discuss the measurement process with the aid of Fig. 1.

In Fig. 1 are presented the two waveforms which must be measured in order to make the transmitted wave start-point determination presently under consideration. The first displayed waveform represents the incident wave as it appears in the transmission region *with the sample panel removed*. Also shown is the transmitted waveform as it is measured with the sample panel in place. (Note that the waveforms are sketched to suggest the dispersive nature of the sample material. In particular, note the different slopes depicted for the initial nonzero values of the incident waveform as compared to those of the transmitted waveform.)
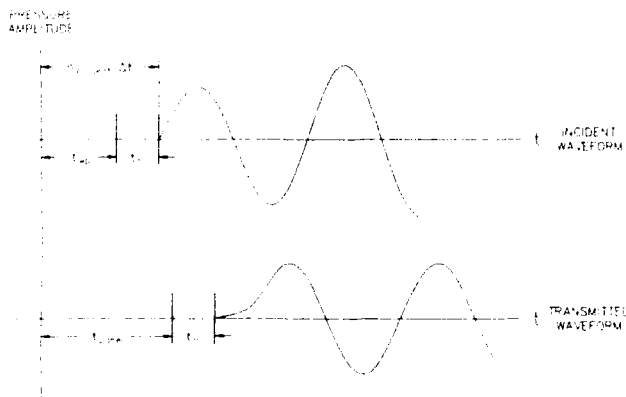

FIG. 1. Waveforms used in determining the start point of the transmitted wave. Here, t = time (where t = 0 is defined to be the arrival time of the incident waveform at the panel interface located closest to the source of the interrogating wave). Δt = digitized sample spacing in the time domain (typically 0.25 μs). $n_{incident}$ = data point number of the start point of the incident waveform as measured in the transmission region with the sample removed. t_{wp} = time of flight of incident wave through water situated in the region where the panel was prior to removal. t_h = time of flight of incident and/or transmitted wave through the water situated between the hydrophone located in the transmission region and the panel interface located farthest from the source of the interrogating wave, and t_{panel} = time of flight of the transmitted wave through the actual material of the sample between the panel interface located closest to the source of the interrogating wave and the panel interface located farthest from the source of the interrogating wave.

The waveforms are displayed with coincident time coordinates, with t = 0 defined to be the arrival time of the incident wave at the "front" panel interface; i.e., the sample surface located closest to the source of the interrogating wave. Each waveform has an associated null region, which is subdivided in the figure into two subregions. The t_{wp} time region is the time of flight of the incident wave in passing through the region of water that is located where the panel was prior to its removal. If we let l denote the overall sample thickness, and let c_w denote the speed of sound in water, then $t_{wp} = l/c_w$. (The value of l is determined in the ONION method with the help of an underwater video camera.)

The t_h time region denotes the time of flight of the incident wave from the "back" panel interface (i.e., the interface farthest from the acoustic source) to the detecting hydrophone in the transmission region. Due to the uncertainty in the location of the effective acoustic center of the hydrophone, this time cannot be reliably determined using a distance measurement of the sort discussed above to determine the quantity t_{wp}. However, the quantity t_h can be determined indirectly, as we will see presently.

For the transmitted waveform, the quantity t_{panel} denotes the (unknown) time of flight of the transmitted wave from the front panel interface to the back panel interface, through the actual material of the sample. The quantity t_h has the same meaning as discussed above in connection with the incident waveform.

Note from Fig. 1 that, in order to make the transmitted waveform appear to have been measured at the back panel interface, the waveform must be shifted (to the "left") by a data-point number that is equivalent to the time t_h. This quantity is determined from the incident-wave measurement in the following way: First, the start point of the incident waveform, as measured in the transmission region, is determined by performing a similar type of statistical comparison of the null part of the waveform with the initial nonzero portion of the waveform as is used to make the first-level start-point determination for the reflected wave. (Of course, this method is significantly more reliable when applied to the incident wave than when it is applied to either the reflected or transmitted wave because of the much greater signal-to-noise ratio of the incident wave.) The data-point number that specifies the start point of the incident waveform as measured in the transmission region with the panel removed is termed $n_{incident}$ in Fig. 1. The quantity Δt of Fig. 1 denotes the sample spacing in the time domain of the digitized waveforms. (Typically, $\Delta t = 0.25$ μs in the ONION method.) The quantity t_h can be determined using the symbols defined here by substitution into the formula $t_h = n_{incident} \Delta t - t_{wp}$ (see Fig. 1), where, as discussed above, $t_{wp} = l/c_w$. Thus the required data-point shift[4,5] of the transmitted wave is given in terms of known quantities by the expression $t_h/\Delta t$, which is equivalent to $n_{incident} - t_{wp}/\Delta t$, or $n_{incident} - l/c_w \Delta t$.

II. THE CAUSALITY PROBLEM AND MODEL IMPROVEMENTS

As was discussed in a previous article,[2] the ONION-method model is noncausal. This difficulty arises from the treatment of the frequency dependence of the sound speed

and loss functions in the model. The model treats the loss function of the panel materials as frequency dependent, but treats the sound speed as frequency independent. This treatment of these functions is inconsistent with the requirements of causality.[6] Although provisions to account for the noncausality of the model are present in the software that implements the ONION-method algorithm, it is nonetheless worthwhile to investigate modifications of the model that can render it consistent with the causality principle. This is particularly important in the present work since it is almost certainly not sufficient to merely deduce "curve-fitting" properties if the simultaneous fitting of reflection and transmission data is desired, as is the case here.

In order to investigate how the ONION model might be rendered consistent with the causality principle, a number of attenuation–dispersion pairs available in the geophysical literature[6-15] were considered. The software that implements the model calculations was modified to successively incorporate each of these literature models. The modified software was then used to analyze panel calibration data. Unfortunately, none of these models proved to be any more successful in fitting the data than the noncausal model originally considered.[1] That is, the mean-squared error of fit between the model and the data was not found to be improved by using these models from the literature.

This result is not as surprising as it might, at first, appear. Although the literature models satisfy the causality principle exactly, this exact behavior is achieved at the cost of assuming a specific (and quite simple) functional form for the loss function. (For example, the model considered by Futterman[13] assumes the loss function varies linearly with frequency.) The sound-speed variation with frequency is then deduced using the appropriate Hilbert transform.[6] This Hilbert transform calculation assures that the causality principle will be satisfied exactly. However, if the experimental data exhibit behavior that is inconsistent with the assumed frequency dependence of the loss function, the model will nonetheless fail to fit the data well.

Of course, considering the manner in which typical panel sublayers are fabricated, subsuming such complexities as voids and seams, there is no compelling reason to suppose that a linear variation, or any other simple functional variation, of the loss function with frequency will be satisfactory.[16] In fact, considering the unknowns involved in sublayer fabrication, such as void size, shape, and distribution, it is unlikely that a simple loss function exists that can accurately accommodate all cases of current, or potential future, interest.

The ONION-method model, despite being noncausal, can accommodate a wide variety of materials due to the fact that no strict assumptions are made in the functional form of the loss function. That is, the loss function is modeled by a Taylor series, with unknown expansion coefficients, truncated at the quadratic term. This model is, of course, compatible with any data that exhibit constant, linear, or quadratic dependence of the loss function on frequency. However, the model is also at least approximately consistent with much more complicated frequency variations, provided that the quadratic-term truncation of the Taylor series yields a rea-

sonable approximation to the true loss function. [Since the frequency content of the interrogating pulses used in the experiments performed to implement ONION-method measurements covers a relatively narrow 0- to 40-kHz band (with no significant information below about 100 Hz), and since the Taylor series is expanded about the steady-state interrogating-wave frequency, this truncated Taylor series is likely to be a reasonable approximation to a wide class of loss functions.] The ability of the model to accommodate a wide variety of loss function frequency variations serves to explain its success in evaluating panel calibration data, despite the inconsistency with the causality principle.

In view of the superior performance of the ONION-method model compared to the literature models in evaluating panel-test data, and considering the fact that no compelling dispersion–attenuation pair is available for the complex materials used in panels, it was decided to abandon at the present time the attempt to render the ONION model strictly consistent with the causality principle. It was decided instead to introduce additional flexibility into the model to at least *permit* causal behavior. This is accomplished in the present version of the ONION-method model by introducing a truncated Taylor series for the frequency variation of the sound-speed function that is similar to that introduced previously for the loss function.

The Taylor series previously introduced to accommodate the frequency variation of the loss function has the form[1]

$$\alpha^{(m)}(\omega) = \frac{1}{\lambda_0^{(m)}}\left(a_0^{(m)} + a_1^{(m)}\frac{(\omega - \omega_0)}{\omega_0} + a_2^{(m)}\frac{(\omega - \omega_0)^2}{\omega_0^2}\right),\tag{1}$$

and the additional Taylor series hereby introduced to better accommodate the frequency variation of the phase speed function is

$$c_{ph}^{(m)}(\omega) = c_{ph}^{(m)}(\omega_0) + \left(b_1^{(m)}\frac{(\omega - \omega_0)}{\omega_0} + b_2^{(m)}\frac{(\omega - \omega_0)^2}{\omega_0^2}\right)c_w.\tag{2}$$

In these equations, ω is the (variable) angular frequency, ω_0 is the (constant) steady-state driving angular frequency of the interrogating wave, $\lambda_0^{(m)}$ is the wavelength of the acoustic wave in the layer of interest at angular frequency ω_0, c_w is the sound speed in water, and $c_{ph}(\omega_0)$ is the sound speed in the layer of interest at ω_0. The parameter m is an integer used to number each layer. The Taylor series expansion constants $a_0^{(m)}, a_1^{(m)}, a_2^{(m)}, c_{ph}^{(m)}(\omega_0), b_1^{(m)}$, and $b_2^{(m)}$ are the parameters that are adjusted using a least-squares fitting process that is similar to that described in Refs. 1 and 2.

In Fig. 2 is presented a block diagram that summarizes the revised ONION method. The method requires two phases. As with the earlier implementation,[1,2] phase 1 of the present implementation uses portions of the reflected time waveform that are free from multiple internal reflections, so that the simple theoretical expressions for the reflection and
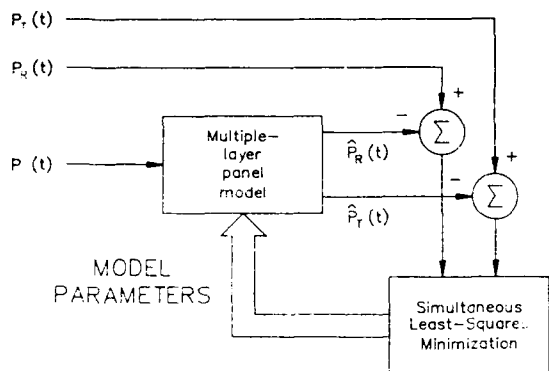
PHASE 1
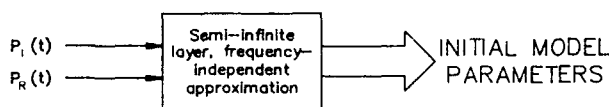
PHASE 2

FIG. 2. Block diagram of revised ONION-method algorithm. As with the earlier implementation (see Refs. 1 and 2), the process requires two phases. Phase 1 represents the "layer-stripping" (or "onion-peeling") phase, during which data that are free from multiple internal reflections are analyzed, using the simple expressions for the reflection and transmission coefficients for two semi-infinite media. This analysis produces approximate sound speeds and losses for each layer. In phase 2, a nonlinear least-squares calculation is used iteratively to improve the approximate parameter values. During this phase, a simultaneous fit of experimental reflected and transmitted waveforms to appropriate model waveforms is performed. Unlike the method of Refs. 1 and 2, the model used in the present implementation includes a Taylor series expansion for the phase-speed function for each layer in addition to that previously used for the loss function. Here, $P_I(t)$ is the experimental pulsed-incident time waveform, $P_R(t)$ is the experimental pulsed-reflected time waveform, and $P_I(t)$ is the experimental pulsed-transmitted time waveform. Similarly, $\hat{P}_R(t)$ is the computed pulsed-reflected time waveform and $\hat{P}_I(t)$ is the computed pulsed-transmitted time waveform, based on applying the transfer function of multiple-layer theory, suitably modified to incorporate the two above-mentioned Taylor series, to $P(t)$.

transmission coefficients for two semi-infinite media in intimate contact are applicable. This calculation is used to deduce approximate starting parameter values. In phase 2 a nonlinear least-squares fitting algorithm is used iteratively to produce improved parameter values. This process produces parameter values that are most consistent (in a least-squares sense) with the available data. In view of the disparate nature of the two sets of waveforms being fitted (i.e., the reflected and transmitted waveforms), the sound speeds and losses obtained in this way are expected to be more reliable estimates of the true effective sound speeds and losses of each layer than are those deduced previously[1] by only fitting reflected-wave data. This will be discussed further in Sec. IV.

It is important at this point to mention that in implementing the simultaneous least-squares minimization process of the phase-2 portion of the algorithm, a weighting

scheme is used to put the two fitted waveforms on an equal footing. That is, since the amplitude of the transmitted wave is often much lower than that of the reflected wave (sometimes more than 40 dB lower), if no account were taken of this lower amplitude then the differences between the model and the data for the transmitted wave would be completely ineffectual in driving the calculations of model corrections. To correct for this, the ratio of the mean-squared amplitude of the reflected wave to that of the transmitted wave is used as a weighting factor to put the two waves on an equal footing. This weighting factor is used in evaluating the contributions of the transmitted-wave data in the least-squares fitting process.[17]
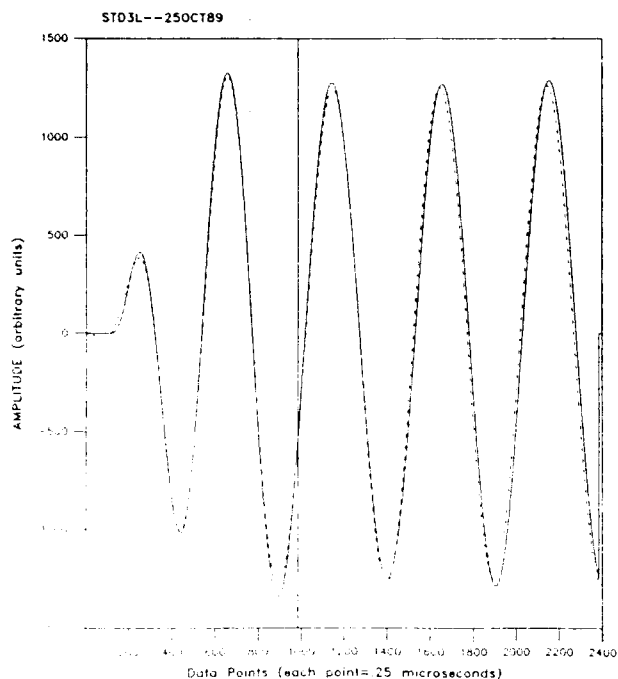
III. EXPERIMENTS

Experimental measurements were undertaken to investigate the effectiveness of the revised ONION method. As was done in the earlier reports,[1,3] tests were carried out on two different samples. One sample contains simple homogeneous layers, while the other contains complex layers fabricated from voided rubbers affixed to a steel backing plate. Measurements performed on the sample containing simple homogeneous layers covered the frequency range 3–10 kHz. Measurements performed on the sample containing voided-rubber sublayers covered the frequency range 1–10 kHz. In both cases, the source-to-sample separation used was 200 cm; sample-to-detector separations were 5 cm from each relevant interface on both the reflected and transmitted sides of the sample. Transmitted waveforms were acquired using a configuration obtained by rotating the sample 180° with respect to the configuration used to obtain the reflected waveforms. As has been observed previously,[18] this configuration (in which the backing plate *faces* the acoustic source) is a better experimental realization of infinite-sample transmitted-wave theory than is the standard configuration (in which the backing plate is located on the side of the panel opposite the acoustic source). That is, fitting errors are found to be less using transmitted waveforms acquired with the backing plate facing the source than when using transmitted waveforms acquired when the backing plate is opposite the source.

The panel containing simple homogeneous layers consists of one layer of polymethylmethacrylate of 2.54-cm (1-in.) thickness, followed by a water layer of 2.54-cm thickness and a steel layer of 0.95-cm (3/8-in.) thickness. The sample containing voided-rubber layers consists of a layer of density 0.78-g/cm³ and 4.84-cm thickness which is laminated onto a second layer of density 0.91-g/cm³ and 4.84-cm thickness, followed by a third layer of density 0.62-g/cm³ and 2.84-cm thickness. The third layer is laminated onto a standard steel support plate of 0.95-cm (3/8-in.) thickness. Both samples have square lateral area, 76 cm (30 in.) on a side.

In Figs. 3 and 4 are presented representative waveforms for each of these samples. In Fig. 3 are presented representative waveforms for the sample containing simple homogeneous layers. Test frequency is 8 kHz. In Fig. 4 are presented

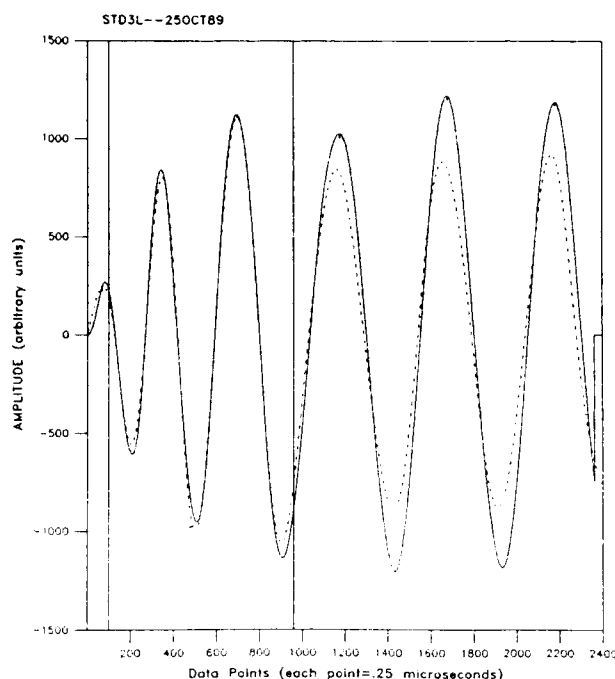Temp: 22.00 Deg C   Press: 110.00 kPa   Freq: 8.00 kHz

Data Window: 1 - 984

STD3L--25OCT89

(a)

Data Points (each point=.25 microseconds)

- - EXTRAPOLATED TRANSMITTED
---- MEASURED TRANSMITTED

Temp: 22.00 Deg C   Press: 110.00 kPa   Freq: 8.00 kHz

Data Window: 100 - 959

STD3L--25OCT89

(b)

Data Points (each point=.25 microseconds)

- - EXTRAPOLATED REFLECTED
—— MEASURED REFLECTED

FIG. 3. Typical experimental and model waveforms for the sample containing three simple homogeneous layers. Frequency is 8 kHz. Solid line—experimental waveforms. Dashed line—numerically computed waveforms based on least-squares fitting to the experimental data available in the indicated data windows. Vertical lines delineate data windows. (a) Transmitted and (b) reflected.

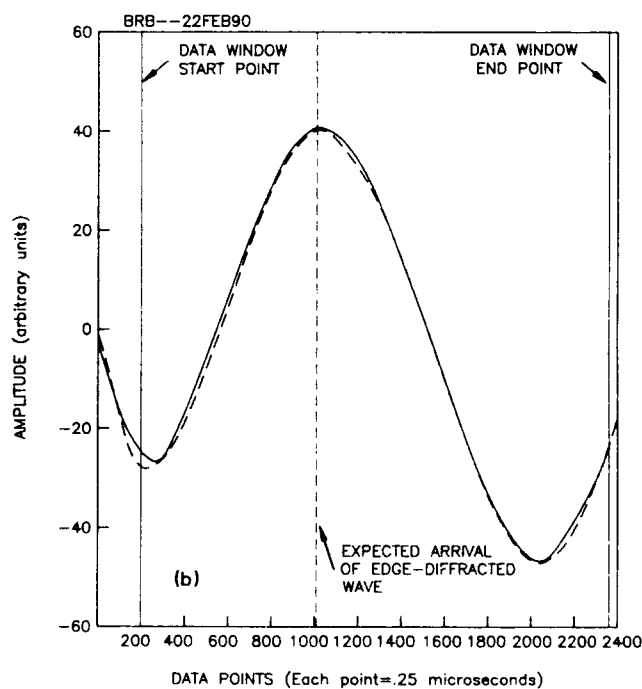TEMP: 21.00 Deg C   PRESS: 110.00 kPa   FREQ: 2.00 kHz

Data Window: 1–2400

BRB--22FEB90

EXPECTED ARRIVAL OF
EDGE-DIFFRACTED WAVE

(a)

DATA POINTS (Each point=.25 microseconds)

—— MEASURED TRANSMITTED
- - - EXTRAPOLATED TRANSMITTED
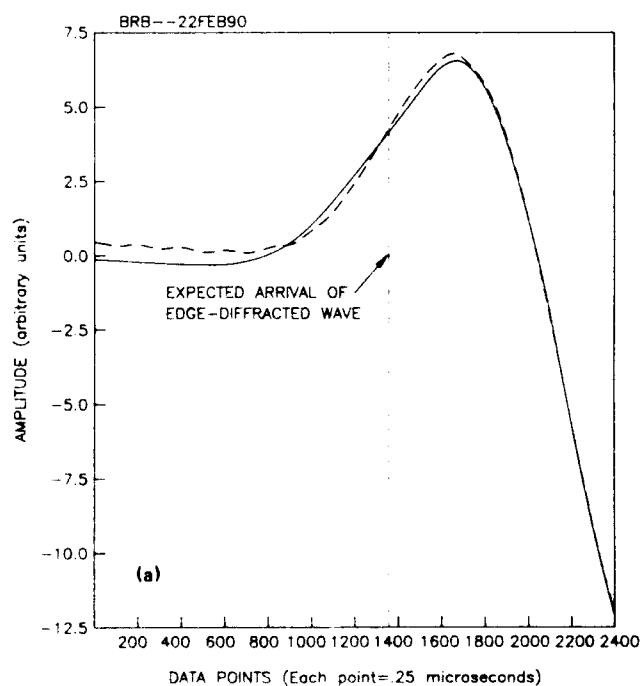
TEMP: 21.00 Deg C   PRESS: 110.00 kPa   FREQ: 2.00 kHz

Data Window: 200–2356

BRB--22FEB90

DATA WINDOW
START POINT

DATA WINDOW
END POINT

EXPECTED ARRIVAL
OF EDGE-DIFFRACTED
WAVE

(b)

DATA POINTS (Each point=.25 microseconds)

—— MEASURED REFLECTED
- - - EXTRAPOLATED REFLECTED

FIG. 4. Same as Fig. 3 except sample is the one containing voided-rubber sublayers and frequency is 2 kHz. Dashed vertical line denotes expected arrival of the edge-diffracted wave. Solid vertical lines in reflected-waveform graph denote start and end points of data analysis window. (The entire depicted transmitted waveform is contained within the data analysis window.) (a) Transmitted and (b) reflected.

representative waveforms for the sample containing voided-rubber sublayers. Test frequency is 2 kHz.

As can be seen, the fit of the model waveforms to the data within the indicated data windows is excellent in both cases. The model waveforms and experimental waveforms for the sample containing simple homogeneous layers can be compared outside the data windows to deduce that edge diffraction is of minor importance in the transmitted wave [note Fig. 3(a)] but is somewhat more significant in the reflected wave [note Fig. 3(b)]. [The same type of comparison cannot be done for the waveforms acquired from the samples containing voided viscoelastic sublayers (i.e., the waveforms of Fig. 4), due to the need to use *all* of the available data in the fitting process. This is necessary due to the very low sound speeds, and greater layer thicknesses, of this sample.] Calculations show that the average root-mean-squared error of fit for the waveforms of Fig. 3 within the data windows is 5.02%, while that for the waveforms of Fig. 4 is 4.31%. These fitting errors are typical of those obtained for the entirety of the data.

In Figs. 5 and 6 are presented graphs that summarize the results obtained for all of the measurements. That is, these graphs present the transmission and reflection coefficients as a function of test frequency for each case. In Fig. 5 are presented results for the sample containing simple homoge-

neous layers. In Fig. 6 are presented results for the sample containing voided-rubber sublayers.

In Tables I and II are presented the material properties deduced for each of these samples at the frequencies used in obtaining the data presented in Figs. 3 and 4, respectively. In Table I are presented results for the sample containing simple homogeneous layers. (The phase speed for PMM that is available in the literature,[19] presented here for comparison, is 2.68×10^5 cm/s.) In Table II are presented results for the sample containing voided-rubber sublayers. Note in Table II that the sound speeds decline with increasing layer number, while losses increase with increasing layer number. Such behavior is a typical design target of panels of this type.

IV. DISCUSSION

We next discuss the reasons it is believed that the material properties deduced by the present method are in fact reasonable estimates of the true material properties of the panel layers. This point of view, of course, is considerably different from that taken in the previous reports[1-3] of work on the ONION method.

First, it is worthwhile to recall the reason that in the earlier reports the material properties obtained were only considered to be "curve-fitting" properties, and not neces-
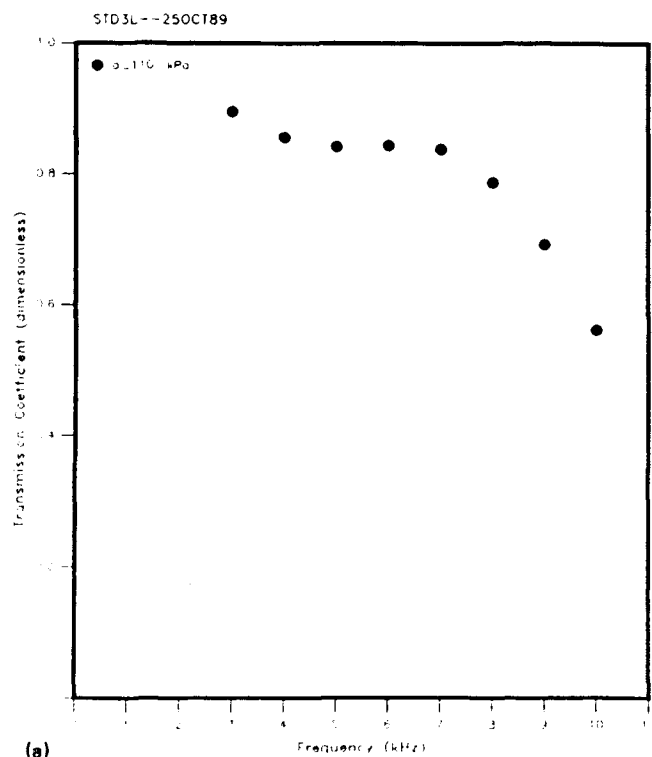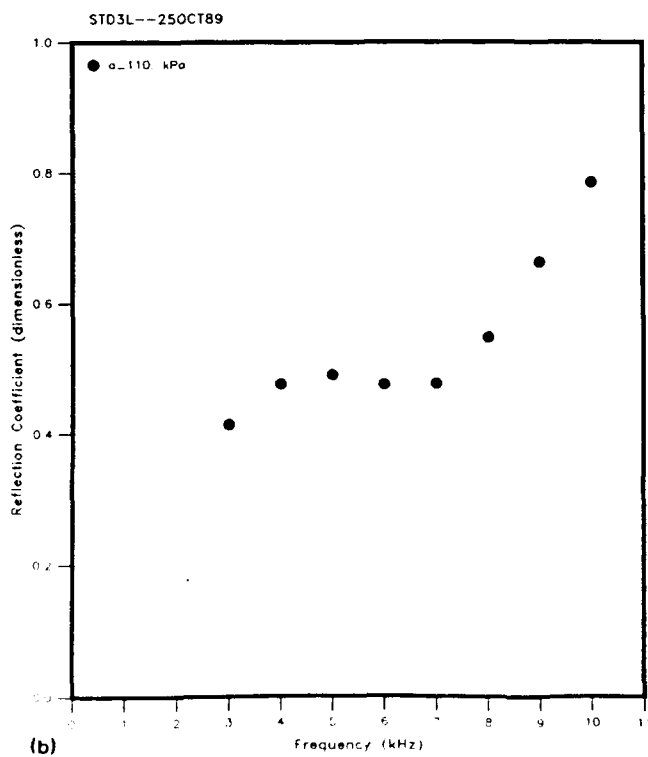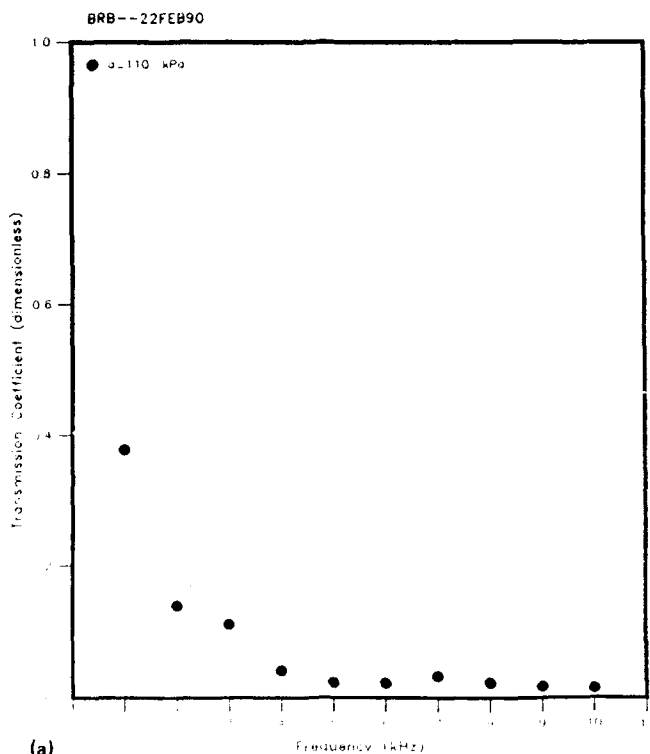

FIG. 5. Coefficients plotted as a function of test frequency for the sample containing three simple homogeneous layers. (a) Transmission coefficients and (b) reflection coefficients.

Transmission Coefficient Summary Graph

Temp: 21.00 Deg C

BRB--22FEB90

(a)

Frequency (kHz)

Reflection Coefficient Summary Graph

Temp: 21.00 Deg C

BRB--22FEB90
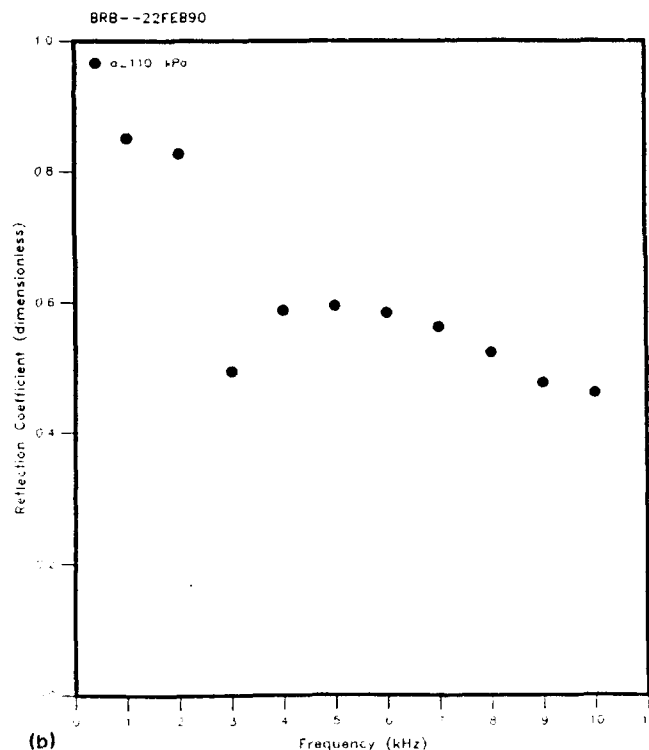

(b)

Frequency (kHz)

FIG. 6. Coefficients plotted as a function of test frequency for the sample containing voided-rubber sublayers. (a) Transmission coefficients and (b) reflection coefficients.

sarily the true sound speeds and losses of the layers. The reason this position was adopted in the earlier work is that it is possible for the reflected return from the panel, especially for layers deep within the panel, to be rather weak. Hence, material properties for the deeper layers can assume a large range of values, and yet a good error of fit between model and data can nonetheless be achieved. In the present work, on the other hand, the requirement to *simultaneously* fit reflected— *as well as transmitted*—wave data severely restricts the parameter space within which the properties of the layers can wander. Note that, unlike the reflected waveform, even the earliest nonzero values of the transmitted waveform have been influenced by *all* the sublayers of the panel. Note further that, if a sound speed for one of the layers were to

wander very far from its true value, an unacceptable phase shift would be introduced into the computed transmitted waveform. That is, the start time of the computed transmitted wave would be incompatible with that of the observed transmitted wave. Hence, a good fit between model and data could not be achieved. Of course, a too-great phase speed for one layer could conceivably be compensated by a too-low phase speed for another layer. However, in this case, it seems unlikely that the resulting waveshape of the computed transmitted wave could properly accommodate that of the measured waveform.

Confidence in the results has also been achieved by attempting certain numerical tests. In one such test, the layer-striping (or onion-peeling) portion of the algorithm was

TABLE I. Material properties deduced for the sample containing simple homogeneous layers. Frequency is 8 kHz. The asterisk denotes that the properties of the steel backing plate were entered *a priori*, and not permitted to vary during the fitting process.

Layer number	c_i (cm/s)	b	b	a	a	a
1	$2.51 \cdot 10$	0.372	0.663	0.0	0.029	0.105
2	$1.41 \cdot 10$	0.117	0.173	0.0	0.0	0.100
3*	$6.1 \cdot 10$	0.0	0.0	0.0	0.0	0.0

TABLE II. Material properties deduced for the sample containing voided-rubber sublayers. Frequency is 2 kHz. The asterisk denotes that the properties of the steel backing plate were entered *a priori*, and not permitted to vary during the fitting process.

Layer number	c_i (cm/s)	b	b	a	a_i	a
1	$5.30 \cdot 10^1$	0.038	0.003	0.0	1.02	0.527
2	$4.32 \cdot 10^1$	0.050	0.004	0.395	1.16	0.530
3	$1.91 \cdot 10^1$	0.045	0.004	1.13	3.78	0.420
4*	$6.1 \cdot 10$	0.0	0.0	0.0	0.0	0.0

over-ridden, and relatively arbitrary starting values of the material properties were used. For example, in one test, involving the data acquired from the sample containing simple homogeneous layers, a phase speed for PMM that is 20% greater than its true value, and a phase speed for water equal to one-half its true value, were used as initial model parameters. Thus the fitting algorithm had every opportunity to wander into wildly inappropriate regions of parameter space in this test. However, the algorithm nonetheless converged to phase speeds for the layers that were within 15% of the true values. Losses were also accurately determined to have a negligible value.

In a second test using these data, the water layer was analytically subdivided into sublayers, with each such sublayer having one-half the true thickness of the layer in question. Each of these sublayers was given an initial sound speed equal to one-half the true sound speed of water, and the properties of each sublayer were permitted to be independently adjusted by the software. The final phase speeds deduced for the two water sublayers were within 5% of each other, and were also each within 15% of the true phase speed of water. (Again, loss was accurately determined to have a negligible value.) Thus the algorithm is seen to be robust against poor initial values for the layer properties.

One final test of the accuracy of the properties deduced by the revised ONION method will be described. In recent tests conducted at our laboratory, a sample panel designed for a decoupling application in an acoustic array was evaluated. The intended application of the panel involves a situation in which a vibrating metal surface in contact with water, but backed by air, is desired to be acoustically isolated. The desired isolation is specified by a velocity-reduction design requirement; i.e., the velocity amplitude on the decoupler surface must be a specified amount smaller than that on the metal surface. The effectiveness of the candidate material in providing the desired isolation was experimentally determined in two ways: (i) using a special test rig consisting of a metallic plate, backed by air, onto which the sample is affixed, and (ii) performing a panel test using the revised ONION method. In (i), the sample material is immersed in water, and a direct observation of the velocity reduction is made. In (ii), a plastic backing plate[18] is affixed to the sample, and the backing plate–sample combination is immersed in water. The velocity reduction for an air-backed metal plate is then deduced by *analytically* removing the plastic backing plate and water backing of test (ii), by using the material properties deduced in (ii) by the revised ONION software, and then analytically inserting an air-backed metal plate. The velocity reduction so obtained is found to be in reasonably good agreement with that obtained from the direct observation in (i). In particular, the two velocity-reduction curves were found to agree to within about 1 dB over a frequency interval exceeding an octave. This agreement is quite good in view of the fact that, due to manufacturing difficulties, the two tested samples were similar but not identical. Such agreement would be unlikely to occur if the material properties used in these calculations were poor estimates of the true material properties.

It will be noted that in the results presented in Figs. 5

and 6 no error bars are given, unlike similar graphs presented previously.[2] The reason for this is that the fitting errors deduced using the standard propagation-of-error methods previously used might not actually provide reliable error estimates. This is due to the fact that there are known sources of systematic error present in the measurements. This systematic error is associated with the rather significant edge-effects that are known to be present in these measurements, especially in the transmitted-wave case. (See Ref. 18). These edge effects are associated with edge diffraction and with surface waves induced in the sample surfaces due to the presence of the sample edges. (Recall that it is necessary to include all the available measured waveform in the transmitted wave analysis due to the low sound-speed and large layer thicknesses of the voided-rubber sample.) The matter of how to properly account for this systematic source of error is the subject of further research.

V. SUMMARY AND CONCLUSIONS

A revised version of the ONION-method software that simultaneously fits reflected- and transmitted-wave data has been described. The revised version incorporates Taylor series expansions of both the loss function and phase-speed function of each panel layer. The modified ONION-method model, despite not being strictly causal, has been found to fit experimental data more accurately than several exactly causal models available in the literature. The material properties deduced for each panel layer by the revised method are believed to be reasonably accurate determinations of these properties, and are no longer regarded as merely being "curve-fitting" properties, as was the case when only the reflected waveform was used as the basis of the least-squares analysis. It is concluded that the revised ONION method provides reasonably accurate determinations of reflection and transmission coefficients, as well as sound speeds and losses for each panel layer, as a function of temperature, pressure, and frequency.

In closing, it is worthwhile to point out that the revised version of the ONION method described in this report has recently been adopted as the standard panel measurement method at the Underwater Sound Reference Detachment of the Naval Research Laboratory (NRL-USRD) in Orlando, FL for panel tests conducted in the 1- to 20-kHz frequency interval.

[1] J. C. Piquette. "An extrapolation procedure for transient reflection measurements made on thick acoustical panels composed of lossy, dispersive materials," J. Acoust. Soc. Am. **81**, 1246–1258 (1987).
[2] J. C. Piquette. "The ONION method: A reflection coefficient measurement technique for thick underwater acoustic panels," J. Acoust. Soc. Am. **85**, 1029–1040 (1989).

[1] J. C. Piquette, "Offnormal incidence reflection coefficient determination for thick underwater acoustic panels using a generalized ONION method," J. Acoust. Soc. Am. **87**, 1416–1427 (1990).

[2] As formulated in the text, the required shift obviously represents a shift of the transmitted waveform to an earlier time (i.e., to the "left"), see Fig. 1. Of course, in a practical measurement, the $t = 0$ reference time of the data-gathering gate will not, in general, correspond to the initial arrival of the incident wave at the front panel interface, as depicted in Fig. 1. Since the actual gate delays are known, they can readily be taken into account (see Ref. 5 below). However, the effect of the gate delays can result in a required shift of the transmitted wave to a later time (i.e., to the "right"), if, for example, the chosen gate start time happens to be less than t_n.

[3] It is also possible that differing time delays, introduced by the electronic measuring apparatus, may be experimentally required to capture each of the two waveforms used in the transmitted-wave shift calculation described here, viz., (i) the transmitted waveform and, (ii) the incident waveform as measured in the transmission region with the sample removed. That is, each waveform might require a different electronic delay in its acquisition. Obviously, an appropriate data-point shift is also required in this case to account for the differing delays.

[4] J. E. White, *Underground Sound* (Elsevier, New York, 1983), pp. 133–138. See especially Eq. (4–66).

[5] B. J. Brennan and D. E. Smylie, "Linear viscoelasticity and dispersion in seismic wave propagation," Rev. Geophys. Space Phys. **19**, 233–246 (1981).

[6] E. Strick, "A predicted pedestal effect for pulse propagation in constant-Q solids," Geophysics **35**, 387–403 (1970).

[7] E. Strick, "The determination of Q, dynamic viscosity and transient creep curves from wave propagation measurements," Geophys. J. R. Astron. Soc. **13**, 197–218 (1967).

[8] P. C. Wuenschel, "Dispersive body waves—an experimental study," Geophysics **30**, 539–551 (1965).

[9] J. E. White and D. J. Walsh, "Proposed attenuation-dispersion pair for seismic waves," Geophysics **37**, 456–461 (1972).

[10] J. C. Robinson, "A technique for the continuous representation of dispersion in seismic data," Geophysics **8**, 1345–1351 (1979).

[11] W. I. Futterman, "Dispersive body waves," J. Geophys. Res. **67**, 5279–5291 (1962).

[12] E. Kjartansson, "Constant Q-wave propagation and attenuation," J. Geophys. Res. **84**, 4737–4748 (1979).

[13] N. Ricker, "The form and laws of propagation of seismic wavelets," Geophysics **18**, 10–40 (1953).

[14] See, for example, G. C. Gaunaurd and W. Wertman, "Comparison of effective medium theories for inhomogeneous continua," J. Acoust. Soc. Am. **85**, 541–554 (1989). See especially Fig. 2.

[15] Readers who are unfamiliar with the handling of weighted observations in a least-squares analysis should consult, e.g., J. B. Scarborough, *Numerical Mathematical Analysis* (Johns Hopkins, Baltimore, 1962), pp. 476–485.

[16] J. C. Piquette, "Technique for detecting the presence of finite sample-size effects in transmitted-wave measurements made on multi-layer underwater acoustic panels," J. Acoust. Soc. Am. **90**, 2831–2842 (1991).

[17] *American Institute of Physics Handbook*, edited by D. E. Gray (McGraw-Hill, New York, 1972), pp. 3–104.

END

FILMED

DATE:
10-92

DTIC